Activation of $GABA_A$ receptors containing the $\alpha 4$ subunit by GABA and pentobarbital

Gustav Akk, John Bracamontes and Joe Henry Steinbach

Department of Anaesthesiology, Campus Box 8054, 660 South Euclid Ave, Washington University, St Louis, MO 63110, USA

The activation properties of $GABA_A$ receptors containing $\alpha 4\beta 2\gamma 2$ and $\alpha 4\beta 2\delta$ subunits were examined in the presence of GABA or pentobarbital. The receptors were expressed transiently in HEK 293 cells, and the electrophysiological experiments were carried out using cell-attached single-channel patch clamp or whole-cell macroscopic recordings. The data show that GABA is a stronger activator of $\alpha 4\beta 2\gamma 2$ receptors than $\alpha 4\beta 2\delta$ receptors. Single-channel clusters were recorded from $\alpha 4\beta 2\gamma 2$ receptors in the presence of 10–5000 μM GABA. The maximal intracluster open probability was 0.35, with a half-maximal response elicited by 32 μM GABA. Simultaneous kinetic analysis of single-channel currents obtained at various GABA concentrations yields a channel opening rate constant of 250 s^{-1}, and a K_D of 20 μM. In contrast, only isolated openings were observed in the presence of GABA for the $\alpha 4\beta 2\delta$ receptor. Pentobarbital was a strong activator of both $\alpha 4\beta 2\gamma 2$ and $\alpha 4\beta 2\delta$ receptors. The maximal cluster open probability, recorded in the presence of 100 μM pentobarbital, was 0.7. At higher pentobarbital concentrations, the cluster open probability was reduced, probably due to channel block. The results from single-channel experiments were confirmed by macroscopic recordings from HEK cells in the presence of GABA or pentobarbital.

(Received 17 November 2003; accepted after revision 13 February 2004; first published online 13 February 2004)
Corresponding author G. Akk: Department of Anaesthesiology, Washington University in St Louis, Campus Box 8054, 660 S. Euclid Ave, St Louis, MO 63110, USA. Email: akk@morpheus.wustl.edu

The $GABA_A$ receptor is a pentameric protein composed of a number of combinations from the 16 subunits cloned so far from the mammalian brain (Rudolph *et al.* 2001). The expression patterns of the subunits differ, allowing a plentitude of differing types of receptor species localized to specific brain regions. The usual form of the receptor is a pentamer of $\alpha\beta\gamma$ or $\alpha\beta\delta$ subunits where the ratio of subunits is normally $2\alpha : 2\beta : 1\gamma$ or δ subunit (Chang *et al.* 1996; Baumann *et al.* 2001).

The expression of the $\alpha 4$ subunit is concentrated in the hippocampus and thalamus where it colocalizes mostly with the $\beta 2$ or $\beta 3$, and $\gamma 2$ or δ subunits (Wisden *et al.* 1992). There seems to be a preference for the δ subunit, with which twice as many $\alpha 4$ subunits assemble compared to the $\gamma 2$ subunit (Sur *et al.* 1999). While the general expression levels for the $\alpha 4$ subunit, and hence the total number of receptors containing this subunit, are relatively low, the functional significance of such receptors may be disproportionally great. A case has been made that the receptors containing the $\alpha 4$ subunit localize mainly to the extrasynaptic regions where they participate in generating tonic current (Nusser & Mody, 2002), thereby controlling the passive membrane properties of the cell (Hausser & Clark, 1997). A high apparent affinity to GABA is a characteristic feature of extrasynaptic receptors, with a concentration producing a half-maximal evoked response of <3 μM (Yeung *et al.* 2003).

Studies of receptors formed after expression of recombinant proteins have demonstrated that the $\alpha 4$ subunit confers distinct pharmacological properties. Such receptors are generally more sensitive to GABA than ones containing the more common $\alpha 1$ subunit (Brown *et al.* 2002). Partial agonists, such as THIP and P4S, are more efficacious on $\alpha 4$ containing receptors, while the receptors containing both the $\alpha 4$ and the δ subunit have been found to be more sensitive to these agonists than ones containing the $\gamma 2$ subunit (Adkins *et al.* 2001; Brown *et al.* 2002). The presence of the $\alpha 4$ subunit does not significantly affect receptor modulation by neuroactive steroids, barbiturates or other anaesthetics (ibid.). However, it has been reported that pentobarbital and propofol are unable to directly activate the $\alpha 4\beta 1\gamma 2$ $GABA_A$ receptor (Wafford *et al.* 1996). Although receptors containing the $\alpha 4$ subunit have distinctive pharmacological properties, there have been only limited quantitative studies of activation of the receptors by GABA or other agonists (Wafford *et al.*

 DOI: 10.1113/jphysiol.2003.058230

1996; Brown *et al.* 2002). Accordingly, to provide a more precise quantitative description of the activation of these receptors by GABA and pentobarbital, we examined single-channel currents. These studies are the initial steps to define the functional differences between the receptors likely to underlie rapid, synaptic inhibitory transmission and those likely to be associated with tonic GABAergic inhibition.

Single-channel kinetic analysis has been used previously to study the biophysical and pharmacological properties of a number of native or recombinant $GABA_A$ receptor subtypes (Twyman *et al.* 1990; Newland *et al.* 1991; Fisher & Macdonald, 1997; Steinbach & Akk, 2001). This approach is particularly well-suited for studies where receptors with known subunit compositions are available, such as in transfection systems. The method allows one to examine the receptor activation properties in detail, and separate a general dose–response curve into components of ligand binding, channel gating and desensitization. The receptors were expressed transiently in HEK 293 cells, and the data were obtained using the cell-attached single-channel patch clamp and whole-cell recording techniques. The results demonstrate that $\alpha 4$ containing receptors are strongly activated by pentobarbital, the efficacy of which is greater at these receptors than that of GABA.

Methods

The $GABA_A$ receptor subunit clones were provided by Drs K. Wafford (human $\alpha 4$), D. Weiss (rat $\beta 1$, $\beta 2$, $\gamma 2L$) and R. Olsen (rat δ). The cDNA was subcloned into a CMV promoter-based vector, pcDNAIII (Invitrogen, San Diego, CA, USA), and used to transfect HEK 293 cells.

Transient transfection of HEK 293 cells using calcium phosphate precipitation was carried out as described earlier (Akk, 2002). In brief, 3.5 μg of cDNA per 35 mm culture dish was used in the ratio of 2 : 2 : 1 ($\alpha : \beta : \gamma$ or δ). The cells were exposed to the precipitate for 14–18 h, after which the medium in the culture dish was replaced. The electrophysiological experiments commenced 24 h after changing the bath medium.

The single-channel currents were recorded using a patch clamp technique in the cell-attached configuration (Hamill *et al.* 1981). The bath solution contained (mM): 140 NaCl, 5 KCl, 1 $MgCl_2$, 2 $CaCl_2$, 10 glucose and 10 Hepes; pH 7.4. The pipette solution contained (mM): 120 NaCl, 5 KCl, 10 $MgCl_2$, 0.1 $CaCl_2$, 20 tetraethylammonium, 5 4-aminopyridine, 10 glucose, 10 Hepes; pH 7.4. Agonists (GABA or pentobarbital) were added to the pipette solution at concentrations indicated in the text. The pipette potential was normally held at +60 to +80 mV. Based on our experience (data not shown), the HEK cell membrane potential is typically −40 mV. Thus, the total potential difference across the patch membrane was between −120 and −100 mV. The channel activity was recorded with an Axopatch 200B amplifier, low-pass filtered at 10 kHz and acquired with a Digidata 1322 Series Interface at 50 kHz using pCLAMP 8 software (Axon Instruments, Foster City, CA, USA). The data were stored on a PC hard drive for further analysis.

In most cases, the kinetic analysis of single-channel currents was restricted to single-channel clusters. A cluster is defined as an episode of intense channel activity which originates from the activation of a single ion channel. A cluster starts when a receptor returns from a long-lived desensitized state and is terminated once the receptor re-enters the long-lived desensitized state. The procedure for identification of $GABA_A$ receptor clusters has been previously described (Steinbach & Akk, 2001). In brief, series of openings isolated from each other by silent periods of at least 250 ms were extracted from the rest of the recording. Episodes containing overlapping currents indicating the activity of two or more receptors were excluded from the analysis. In general, episodes shorter than 250 ms were not included in cluster analysis.

The single-channel clusters were low-pass filtered at 2–4 kHz, and the data were idealized using the segmented-k-means algorithm (Qin *et al.* 1996). The intracluster open and closed times were estimated from histogram fitting using maximum likelihood methods which incorporated a correction for missed events (Qin *et al.* 1996). The open interval duration histograms were initially analysed by fitting a simple C ↔ O model. The number of open states was then increased progressively as long as the increase in the log-likelihood justified the addition of the extra state (Horn, 1987). The open states were connected directly to the closed state, and unconnected to each other. The closed interval duration histograms were analysed in a similar fashion, starting with an O ↔ C model and adding closed states until the addition of more closed states did not significantly improve the fit. Error limits were estimated from the curvature of the likelihood surface as previously described (Qin *et al.* 1997). Cluster open probability, calculated as the fraction of time the receptor spends in the open states within a cluster, and plotted as a function of agonist concentration, is used as the variable in the single-channel concentration–response curve.

In certain cases, receptor activation did not result in single-channel clusters (e.g. $\alpha 4\beta 2\delta$ activated with GABA). Then, 0.5–2 s episodes of single-channel activity were isolated from the recording, and the current open times were analysed as described above. However, no studies

on the current closed times were undertaken for these patches.

The currents arising from the $\alpha\beta\gamma$ and $\alpha\beta\delta$ receptors were distinguished from activity of receptors containing just $\alpha\beta$ subunits according to single-channel conductance, which is approximately 50% greater in the $\alpha\beta\gamma/\alpha\beta\delta$ configuration (Puia *et al.* 1990; Fisher & Macdonald, 1997; G. Akk, unpublished data). During visual inspection, the majority of currents belonged to the high-conductance class, suggesting that $\alpha\beta$ receptors did not contribute significantly to the electrophysiological responses (data not shown).

The pipette solution in whole-cell macroscopic recordings contained (mM): 140 CsCl, 4 NaCl, 4 $MgCl_2$, 0.5 $CaCl_2$, 5 EGTA, 10 Hepes; pH 7.3. Agonists were applied using a gravity-fed delivery system consisting of seven lines entering a single manifold (Fletcher & Steinbach, 1996). The cells were clamped at −50 mV. No compensation for series resistance was carried out. The currents were filtered at 5 kHz and digitized at 100 μs per point. The analysis was carried out using Clampfit 8 (Axon Instruments) software.

Results

Activation of $\alpha4\beta2\gamma2$ receptors by GABA

Receptors containing the $\alpha4$, $\beta2$ and $\gamma2$ subunits are activated in the presence of GABA. Single-channel clusters were observed at GABA concentrations as low as 10 μM. As the agonist concentration was raised, the cluster open probability (P_o) increased. Shown in Fig. 1 are sample clusters elicited by 20 and 1000 μM GABA. The 50-fold increase in GABA concentration results in a notably higher P_o of a cluster.

The intracluster open time (OT) histograms contained three components. We did not observe systematic GABA concentration-dependent changes in the durations or fractions of any of the open time components, suggesting that all openings arise from fully liganded receptors (Fig. 2*A* and *B*). The shortest-lived component (OT_1) had a mean duration of 0.35 ± 0.09 ms and a relative weight of 34 ± 13%. These values are averages from eight patches recorded at 10–5000 μM GABA. The majority of open events belonged to an intermediate duration class (OT_2), having a mean duration of 1.3 ± 0.4 ms and a relative weight of 63 ± 12%. Finally, there was a minor component (OT_3), making up only 3 ± 3% of all intracluster open times, with a mean duration of 6.3 ± 3.8 ms. Due to its greater prevalence, the major portion (75%) of the current is carried by openings belonging to the OT_2 class.

The intracluster closed time (CT) histograms were fitted using a kinetic model in which a single open state was connected to three or four closed states (see Methods), depending on the concentration of GABA. The individual time constants and the rates of entry into the closed states at 10–5000 μM GABA are given in Table 1. Table 1 contains data obtained from one patch

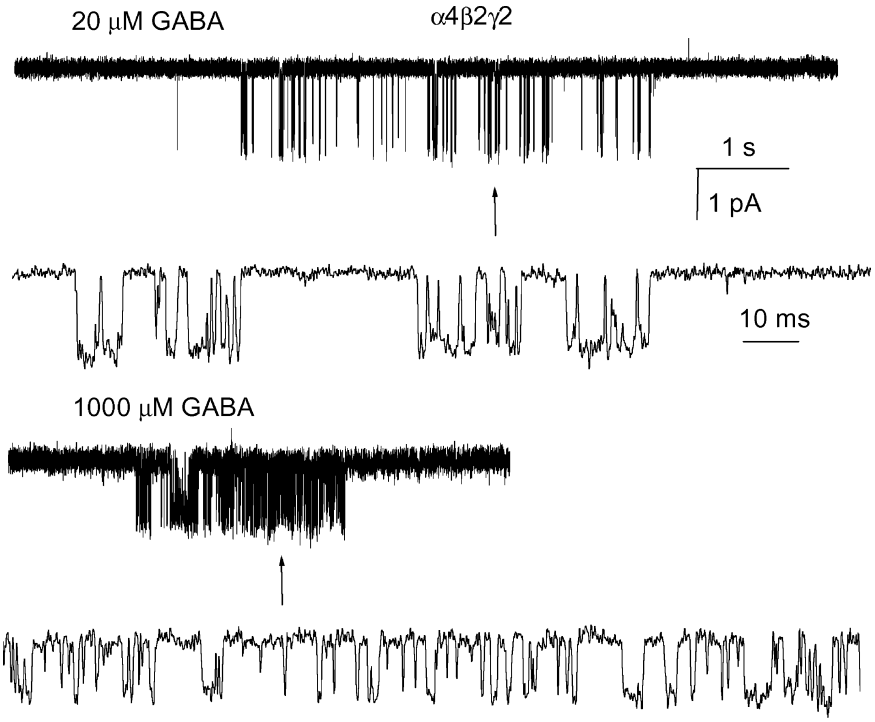

Figure 1. Single-channel clusters from the $\alpha4\beta2\gamma2$ GABA$_A$ receptor
The clusters were elicited by 20 μM (upper traces) or 1000 μM (lower traces) GABA. High resolution fragments are shown below the clusters. Channel openings are shown downward. GABA at 1000 μM elicits a maximal response from this receptor. The intracluster open and closed time distributions are given in Fig. 2 and Table 1, respectively.

per agonist concentration. However, qualitatively similar results were obtained in other patches from different cells (data not shown). The data demonstrate the following. At all agonist concentrations, there is a short-lived closed time component with a mean duration of 0.32 ± 0.09 ms (CT_1, averaged from data from eight patches at 10–5000 μM GABA). This component forms 22 ± 9% of intracluster closed times. In the presence of high (500–5000 μM) and low (10 μM) concentrations of GABA, we observed a relatively long-lived closed state (CT_{SD}, closed time corresponding to a short-lived desensitized state). The mean duration of this closed time component was 19.0 ± 5.1 ms, with a relative frequency of 1 ± 1%. This closed interval is similar, in terms of frequency and duration, to a closed state observed previously and thought to originate from receptor desensitization (Jones & Westbrook, 1995). At GABA concentrations up to 500 μM, a closed state with a mean duration of 1.7 ± 0.3 ms and a relative weight of 66 ± 7% was observed (CT_2). Finally, a closed state of variable duration was observed in the recordings (CT_β, closed time corresponding to activation-related states). The duration of CT_β was similar to CT_{SD} at low GABA concentrations, and practically indistinguishable from that of CT_2 at high GABA concentrations. The relative weight of CT_β could be determined independently under two conditions: at 10 and 500 μM GABA. At 10 μM GABA, the duration of CT_β was much greater than that of CT_{SD}, thereby allowing the separation between the two. Similarly, at 500 μM GABA, the duration of CT_β was intermediate between CT_2 and CT_{SD}, again allowing us to distinguish it from other components. At other GABA concentrations, the duration of CT_β was similar to that of CT_2 or CT_{SD}, preventing the separation of the components. In such cases, the CT_β component merged with the CT_2 or CT_{SD} closed time components, effectively increasing the fraction of the composite state. At 10 and 500 μM GABA,

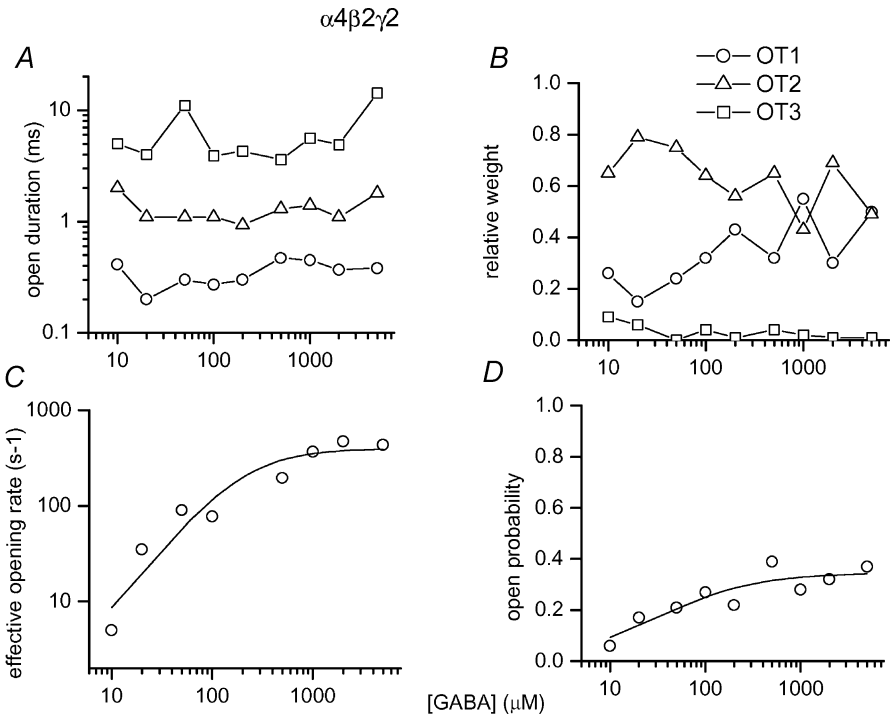

Figure 2. The properties of currents from the $\alpha4\beta2\gamma2$ $GABA_A$ receptor elicited by GABA
A, mean open durations of the three open time components at 10–5000 μM GABA. The durations of open times are not affected by GABA concentration. The averaged open times are: 0.35 ms for OT_1, 1.3 ms for OT_2 and 6.3 ms for OT_3. *B*, relative weights of the three open time components. The relative weights were not affected by the concentration of GABA. The averaged weights are: 34% for OT_1, 63% for OT_2 and 3% for OT_3. The inset key applies to *A* and *B*. *C*, the effective opening rate at various GABA concentrations. The effective opening rate is calculated as an inverse of CT_β (see Table 1). The curve was fitted using a Hill equation. The fitting parameters are : $\beta'_{max} = 399\ s^{-1}$, $EC_{50} = 204\ \mu M$, $n_H = 1.3$. *D*, the intracluster open probability at various GABA concentrations. The curve was fitted using a Hill equation. The fitting parameters are : $P_{o,max} = 0.35$, $EC_{50} = 32\ \mu M$, $n_H = 0.9$. In all panels, each data point corresponds to data from one patch. The numbers of events and clusters used in the analysis are given in Table 1.

Table 1. Parameters for components fitted to the intracluster closed time distributions for currents from $\alpha4\beta2\gamma2$ receptors activated by GABA

[GABA] (μM)	CT_1 (ms)	k_1 (s^{-1})	CT_2 (ms)	k_2 (s^{-1})	CT_{SD} (ms)	k_{SD} (s^{-1})	CT_β (ms)	k_β (s^{-1})
10	0.14 ± 0.05	68 ± 15	1.4 ± 0.1	404 ± 18	12.5 ± 3.6	17 ± 7	200 ± 16	76 ± 6
20	0.43 ± 0.19	156 ± 76	1.6 ± 0.1	600 ± 76	—	—	28.6 ± 1.6	124 ± 7
50	0.30 ± 0.06	133 ± 23	1.8 ± 0.1	791 ± 23	—	—	11.1 ± 0.5	186 ± 11
100	0.38 ± 0.04	387 ± 33	2.1 ± 0.2	575 ± 28	—	—	13.0 ± 1.0	104 ± 13
500	0.32 ± 0.08	212 ± 55	1.5 ± 0.2	616 ± 44	19.2 ± 5.9	5 ± 3	5.1 ± 1.2	82 ± 40
1000	0.38 ± 0.04	262 ± 19	—	—	25.0 ± 3.8	17 ± 3	2.7 ± 0.1	731 ± 20
2000	0.37 ± 0.04	210 ± 19	—	—	19.2 ± 2.2	12 ± 2	2.1 ± 0.04	880 ± 21
5000	0.25 ± 0.03	272 ± 22	—	—	14.3 ± 3.3	21 ± 8	2.3 ± 0.1	567 ± 24

Data were fitted with three or four exponential components. The results of the fits were classified as described in Results. The table gives the time constants for the components CT_1, CT_2, CT_{SD} and CT_β (in ms), and the rates of occurence for each component (in s^{-1}). Data from one patch at each concentration were analysed. At 10 μM GABA the total number of events was 2583 (13 clusters), at 20 μM, 5624 events (13 clusters), at 50 μM, 16510 events (30 clusters), at 100 μM, 11716 events (28 clusters), at 500 μM, 5129 events (14 clusters), at 1000 μM, 11128 events (8 clusters), at 2000 μM, 23092 events (27 clusters) and 5000 μM, 3506 events (10 clusters).

CT_β made up 13 and 9% of intracluster closed intervals, respectively.

We could also predict the fraction of CT_β if we assumed that the longest-lived closed time component observed at 20–100 μM combined both the CT_β and CT_{SD} components, while the longest-lived component observed at 500–5000 μM GABA contained only the CT_{SD} component. Such assumptions can be made because at GABA concentrations equal to and above 500 μM the duration of CT_β is less than the duration of CT_{SD}, allowing the separation of the two closed time components. By subtracting the relative proportion of the longest-lived closed time component at 500–5000 μM from its proportion observed at 20–100 μM, we can estimate the relative fraction of CT_β. The fraction of CT_β estimated using this approach is 13%, agreeing well with our estimates using the data obtained at 10 and 500 μM GABA.

The CT_β state has been associated with dwells in the mono- and unliganded states due to its dependence on the nature and concentration of the agonist (Steinbach & Akk, 2001). The inverse of CT_β at different agonist concentrations, defined as an effective opening rate (β'), is shown in Fig. 2*C*. The curve was fitted using a Hill equation, yielding a maximal effective opening rate (β) of 399 ± 127 s^{-1}, an EC_{50} of 204 ± 155 μM, and a Hill slope of 1.3 ± 0.3. The effective opening rate curve saturates at the value corresponding to the true opening rate constant of the ion channel. Hence, using this approach, the channel opening rate constant of the $\alpha4\beta2\gamma2$ subunit-containing receptor, in the presence of GABA, is estimated as ~400 s^{-1}. The Hill slope value of more than 1 indicates that the binding of more than one agonist molecule is required for activation.

The durations or fractions of CT_1, CT_2 and CT_{SD} are not affected by the concentration of GABA. While the true molecular origin of these states is unknown, it is not likely that they form part of the activation pathway, i.e. dwells in the monoliganded or unliganded states. Similar non-conducting states have been observed previously for the recombinant $\alpha1\beta\gamma2$ receptor ($\beta1$, Haas & Macdonald, 1999; $\beta2$, Steinbach & Akk, 2001) and in native $GABA_A$ receptors from mouse spinal cord neurones (Twyman *et al.* 1990) or cultured hippocampal neurones (Jones & Westbrook, 1995).

In the absence of a generally accepted $GABA_A$ receptor activation model, another approach to determine the channel opening rate constant, and to get an estimate for the receptor affinity, is to fit a model in which a single open state is connected with closed states associated with agonist binding and the three agonist-independent closed states to the single-channel data obtained at several GABA concentrations:

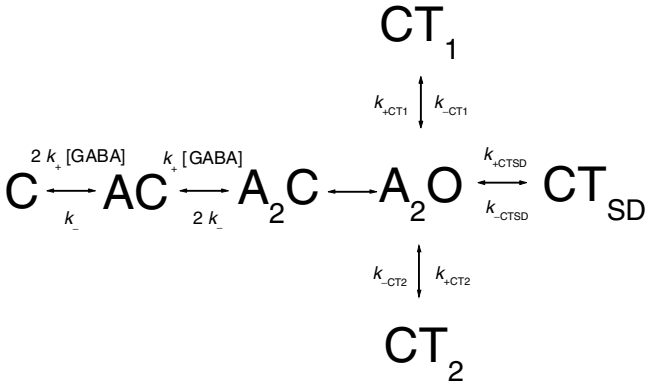

Model 1

In this model, the transitions between the open state (A_2O) and CT_1, CT_2 or CT_{SD} are independent of GABA concentration. The pathway from C (unliganded, closed state) to A_2O corresponds to the CT_β component in the closed time histograms. This pathway consists of two agonist binding steps, and a step corresponding to the conformational change of the diliganded, closed receptor (marked with β). The conformational change is unaffected by the agonist concentration, being the limiting value for the CT_β component at saturating GABA concentrations. It should be mentioned that no assumptions regarding the true activation model have been made here other than that (i) two agonist binding steps are required for channel opening, (ii) all three open states observed in the recordings behave essentially similarly to the single composite open state shown in Model 1, and (iii) states corresponding to closed time components CT1, CT_2 and CT_{SD} are not part of the activation pathway. Some or all of these closed states may actually originate from the A_2C state.

We used the QuB suite (www.qub.buffalo.edu) to fit Model 1 to the single-channel data obtained in the presence of 20, 100 and 5000 μM GABA (one patch at each concentration containing 5624, 11716 and 3506 events, and 13, 28 and 10 clusters, respectively). The dead time was set at 72 μs. The GABA concentrations were chosen to fully cover the low and high ends of the concentration–response curves (Fig. 2*C* and *D*). In the simultaneous fitting of the three files, the only constraint was to assume that the two agonist binding sites have equivalent affinities to GABA. It should be mentioned that there are no data suggesting that the GABA binding sites have equal K_D values; this constraint was used simply to reduce the number of free parameters. The results of the fit are as follows. The agonist association rate constant (k_+) is $5 \pm 1\,\mu M^{-1}\,s^{-1}$, the agonist dissociation rate constant (k_-) is $100 \pm 26\,s^{-1}$, yielding a K_D of 20 μM. The channel opening rate constant (β), estimated from Model 1, is $250 \pm 32\,s^{-1}$, and the channel closing rate constant (α) is $218 \pm 69\,s^{-1}$. The rates of entry into and return from the blocked/desensitized states are: for CT_1, $k_{+CT1} = 224 \pm 83\,s^{-1}$ and $k_{-CT1} = 3894 \pm 387\,s^{-1}$, for CT_2, $k_{+CT2} = 526 \pm 40\,s^{-1}$ and $k_{-CT2} = 666 \pm 49\,s^{-1}$, and for CT_{SD}, $k_{+s.d.} = 16 \pm 4\,_s^{-1}$ and $k_{-s.d.} = 39 \pm 5\,s^{-1}$. Figure 3 shows the closed interval duration histograms for the three patches used in the analysis, and the interval duration distributions as predicted from the rate constants estimated using Model 1.

Thus, two approches were used to estimate the channel opening rate constant in the presence of GABA. Fitting the inverse duration of CT_β to the Hill equation gave $399\,s^{-1}$, while fitting Model 1 to currents recorded at three GABA concentrations yielded $250\,s^{-1}$ for the channel opening rate constant. The discrepancy between the two estimates is probably due to imprecise determination of CT_β when its duration falls close to other components in the closed interval distribution.

The intracluster open and closed times determine the cluster open probability. The intracluster open probability *versus* GABA concentration relationship is given in Fig. 2*D*. The curve was fitted with the Hill equation, yielding a maximal open probability of 0.35 ± 0.04, an EC_{50} of 32 ± 16 μM and a Hill coefficient of 0.9 ± 0.4.

Activation of $\alpha4\beta2\gamma2$ receptors by pentobarbital

We next studied receptor activation by pentobarbital (PB). Within the concentration range 10–1000 μM PB, activation of $\alpha4\beta2\gamma2$ receptors occurred in single-channel clusters. Sample clusters obtained in the presence of 200 and 1000 μM PB are shown in Fig. 4*A* and *B*. Comparison of the two clusters demonstrates a typical characteristic

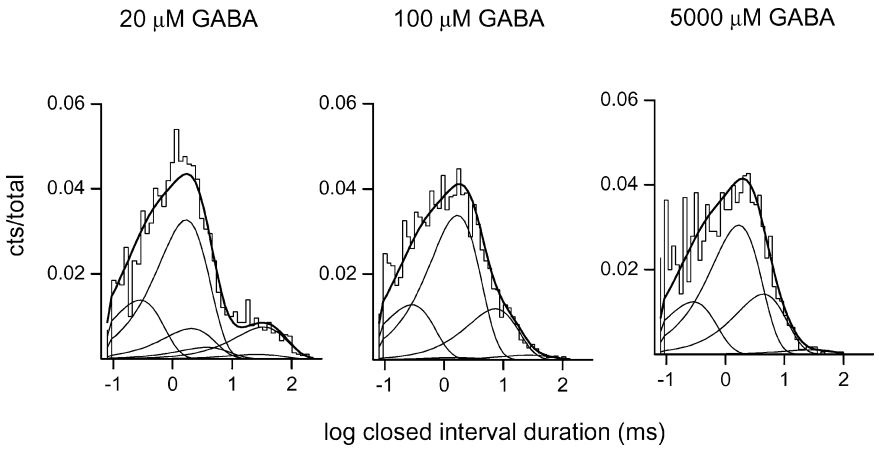

Figure 3. The intracluster closed time histograms from $\alpha4\beta2\gamma2$ subunit receptors activated by 20, 100 and 5000 μm GABA
The continuous lines were calculated according to Model 1 and the rate constants given in the text. The numbers of events and clusters used in the analysis are given in the text.

of PB-mediated activation – a decrease in the channel open probability at high PB concentrations due to channel block. A similar effect of high concentrations of PB has been previously described for the $\alpha1\beta2\gamma2$ receptor (Akk & Steinbach, 2000). Figure 4*C* gives the intracluster open probability obtained at various PB concentrations. The data demonstrate a decline in cluster open probability at PB concentrations above 200 μM caused by a decline in the open time durations (Fig. 4*D*) and an increase in the mean intracluster closed interval duration (Fig. 4*E*). The cluster open probability at 30–200 μM PB is higher than the maximal open probability in the presence of GABA (Fig. 2*D*), indicating that PB is a higher efficacy agonist at the $\alpha4\beta2\gamma2$ receptor.

The number of open time components and the durations of the individual components were affected by the concentration of PB. At 200 μM PB, the intracluster open time histograms contained three components similar to what was observed in the presence of GABA. The components had the mean durations (relative frequencies) as follows (estimated from a total of 6305 events): for OT_1, 0.18 ± 0.02 ms (20 ± 1%); for OT_2, 1.9 ± 0.2 ms (13 ± 6%); for OT_3, 5.8 ± 0.3 ms (67 ± 6%). Thus, the majority of openings belonged to the long-lived component class, in contrast to activity elicited by GABA. In currents obtained at higher PB concentrations, the number of components in the open time histograms was reduced. At 500–1000 μM PB, the OT_3 component was absent while at 2 mM PB, only one component remained in the open time histograms. The two components observed at 500–1000 μM PB were similar to OT_1 and OT_2 in terms of durations. The relative frequency of the shorter-duration component at 500 μM PB (13%) was similar to that of OT_1 observed at 200 μM. At 2 mM PB, the single open time component had a duration of 0.63 ± 0.02 ms (1818 events). This value is intermediate between those for OT_1 and OT_2 observed at lower PB concentrations.

The intracluster closed time durations increased when the PB concentration is raised above 200 μM. The mean closed time was 2.5 ± 0.04 ms at 200 μM, 6.4 ± 0.1 ms (5643 events) at 500 μM and 8.9 ± 0.2 ms (4115 events) at 1 mM PB. The trends observed in the open and closed times are similar to what was observed previously for the $\alpha1\beta2\gamma2$ subunit-containing receptor where the increase in the channel closed time durations and the decrease in the channel open time durations were associated with PB-mediated channel block (Akk & Steinbach, 2000).

Figure 4*D* shows the relationship between the mean open duration and the concentration of PB. As PB concentration is increased, the mean open duration is decreased. The continuous line was fitted to: $OT = 1/(\alpha + k_{+B}[PB])$, where α is the true channel closing rate constant and k_{+B} is the channel blocking rate constant. According to the fit, $k_{+B} = 0.59 \pm 0.27\ \mu M^{-1}\ s^{-1}$ and $\alpha = 134 \pm 24\ s^{-1}$. In this fit, no consideration was given to the presence of the multiple open time components. The value for k_{+B} is similar to one obtained previously for the $\alpha1\beta2\gamma2$ receptor ($0.56\ \mu M^{-1}\ s^{-1}$; Akk and Steinbach, 2000) suggesting that the site involved in the PB blocking mechanism remains intact when the $\alpha1$ subunit is replaced by the $\alpha4$ subunit.

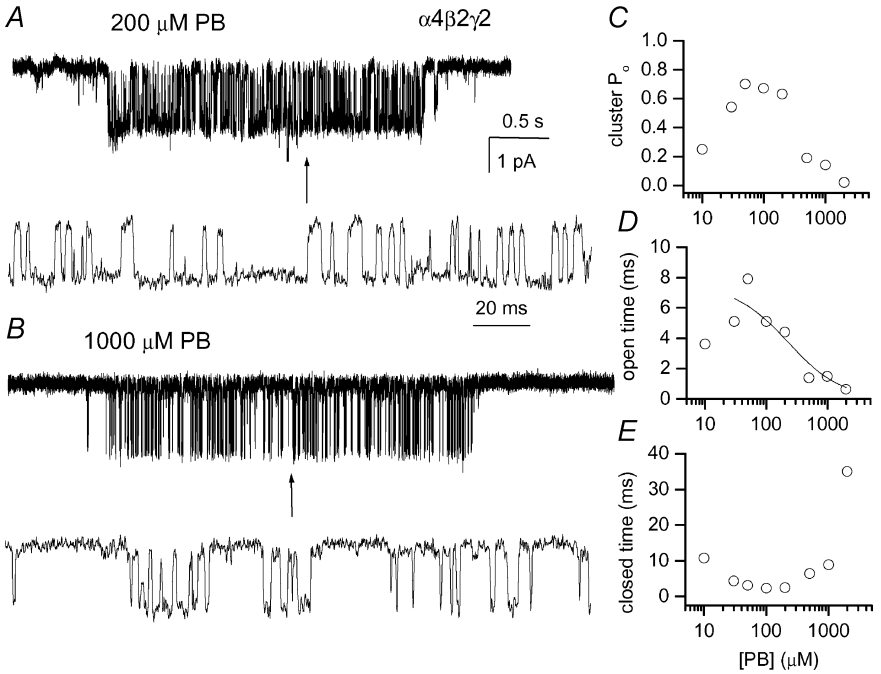

Figure 4. Single-channel clusters from the $\alpha4\beta2\gamma2$ $GABA_A$ receptor
The clusters were elicited by 200 μM (*A*) or 1000 μM (*B*) pentobarbital. Higher resolution fragments are shown below the clusters. Channel openings are shown downward. PB at 200 μM elicits a maximal response from this receptor; at higher concentrations PB inhibits the receptor function. *C*, the intracluster open probability at various PB concentrations. *D*, the calculated mean open interval duration at various PB concentrations. The curve was fitted using an equation: open time = 1/(closing rate + k_{+B}[PB]). The fitting parameters are: closing rate = 134 ± 24 s^{-1}, $k_{+B} = 0.59 \pm 0.27\ \mu M^{-1}\ s^{-1}$. Only data obtained at 30–2000 μM PB were used in the analysis. *E*, the calculated mean closed interval durations at various PB concentrations.

The calculated mean closed time in a cluster decreased with increasing PB concentrations from 10 to 100 μM, as would be expected for an agonist. The observation that the mean closed time increased with PB concentration above 100 μM suggests that more than one PB molecule can be involved in block, as was suggested previously for the $\alpha1\beta2\gamma2$ receptor (Akk & Steinbach, 2000) and the $\alpha1\beta2$ receptor (Serafini *et al.* 2000).

Macroscopic currents from $\alpha4\beta2\gamma2$ receptors activated by GABA and pentobarbital

We also studied the activation of $\alpha4\beta2\gamma2$ receptors using whole-cell voltage clamp. The reason for doing these experiments was to confirm receptor activation by PB under non-equilibrium conditions, such as during a pulse of agonist application. It has been proposed that different kinetic states are occupied during different phases of macroscopic currents (Haas & Macdonald, 1999). The steady-state single-channel currents may be related to the residual currents in the end of a prolonged pulse of agonist application. Therefore, we were interested in comparing the amplitudes of peak currents under non-equilibrium conditions during receptor activation by GABA or PB.

The results from the whole-cell experiments demonstrate that PB is a strong activator of the $\alpha4\beta2\gamma2$ receptor. The peak currents obtained in response to applications of 100 μM PB were higher than those recorded in the presence of 1 mM GABA (Fig. 5*A* and *B*). Both agonist concentrations represent the conditions under which maximal responses were elicited during steady-state single-channel patch clamp. Thus, the macroscopic peak currents qualitatively agree with the findings from the single-channel experiments demonstrating that PB is a higher efficacy agonist than GABA on the $\alpha4\beta2\gamma2$ receptor. The whole-cell currents elicited by 1 mM GABA compared to that elicited by 100 μM PB (85%) were somewhat larger than expected based on cluster open probability (0.4/0.7 = 56%).

High concentrations of PB (= 1 mM) led to block of the receptor, as witnessed by the depression of peak current and the development of rebound currents in the end of PB application. The rebound currents result from the release of block when the occupied, blocked receptors return to the unliganded form via an open state (Akaike *et al.* 1987).

Residual current levels were estimated during an agonist application 5 s after the peak. These values were used to evaluate receptor desensitization in the presence of PB or GABA. Figure 5*C* gives the residual current levels in the presence of 100 or 1000 μM PB, or 1 mM GABA. The results indicate only relatively minor desensitization ($<$ 40%) taking place within 5 s. It should be noted, however, that steady-state levels were not reached within 5 s for receptors activated by 100 μM PB.

We have compared the current levels in the presence of 10– 2000 μM PB as estimated from the single-channel and whole-cell experiments. The parameter used for single-channel currents was cluster open probability (see above), while for whole-cell currents, the amplitude of the peak current was used. In both cases, the values for current levels were normalized to that observed in

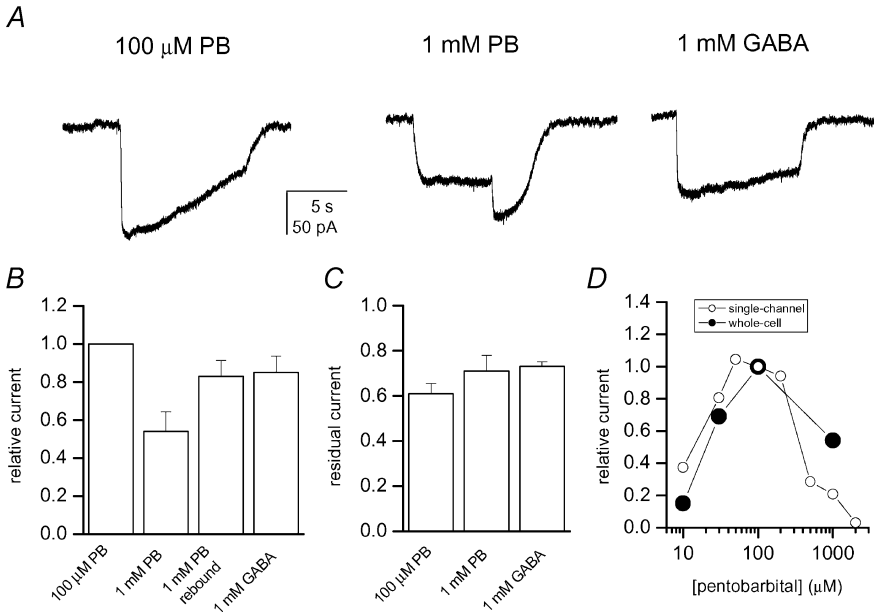

Figure 5. Macroscopic currents from HEK cells expressing $\alpha4\beta2\gamma2$ subunit receptors
A, the currents were elicited by 100 μM PB, 1 mM PB or 1 mM GABA. Rebound current in the end of the 1 mM PB application is caused by removal of PB-mediated block. *B*, normalized to peak current levels in the presence of 100 μM PB, the relative peak current for 1 mM PB was 0.54 ± 0.23 (n = 5), for 1 mM PB the rebound current was 0.83 ± 0.19 and the peak current for 1 mM GABA was 0.85 ± 0.21 (n = 6). *C*, residual current measured 5 s after the peak response is plotted. The residual current level for 100 μM PB was 0.61 ± 0.11, for 1 mM PB it was 0.71 ± 0.14 and for 1 mM GABA it was 0.73 ± 0.05. *D*, comparison of single-channel cluster open probability and peak macroscopic responses in the presence of pentobarbital. The currents were normalized to the levels at 100 μM PB.

the presence of 100 μM PB. Shown in Fig. 5*D* are the relative current levels as estimated from single-channel and whole-cell experiments. With both methods, a bell-shaped relationship between the relative current and the concentration of PB is detected, with maximal current levels observed at ~50–100 μM PB.

Single-channel and macroscopic currents from α4β2δ receptors elicited by GABA and pentobarbital

Finally, we also studied the activation of α4β2δ receptors by GABA and PB. In the presence of GABA, the activity of α4β2δ receptors takes place as isolated openings with no apparent desensitization-delimited single-channel clusters. Shown in Fig. 6*A* are sample currents elicited by 1000 μM GABA. The channel open events were fitted with a sum of two exponentials (to a total of 1406 events), with the time constants of 0.12 ± 0.03 ms and 3.2 ± 0.1 ms. The longer-duration openings were four times as prevalent as the shorter duration openings. Due to the absence of single-channel clusters, no further analysis was carried out on α4β2δ receptors activated by GABA.

We next studied the activation of α4β2δ receptors by 10–200 μM pentobarbital (PB). In contrast to what was observed in the presence of GABA, PB was a strong activator of the α4β2δ receptor. Groups of channel openings with high open probability were observed at PB concentrationsof 40 μM (Fig. 6*B*). The open time histograms from such groups obtained in the presence of 40 μM PB contained three components. The mean durations (relative frequencies) of the components were (3913 events): for OT_1, 0.11 ± 0.02 ms (10 ± 1%); for OT_2, 1.5 ± 0.4 ms (13 ± 2%); for OT_3, 11.1 ± 0.4 ms (77 ± 4%). Therefore, similarly to the α4β2γ2 receptor, the channel open times are prolonged in the presence of low concentrations of PB compared to GABA.

PB at higher concentrations appeared to block the channel openings. This resulted in the loss of the longest-lived component, OT_3 from the open time histograms at PB concentrations of 100 μM and above, and the subsequent reduction in the duration of OT_2. The calculated mean open time durations were 9.2 ms with 40 μM PB, 4.6 ms with 100 μM PB and 3.3 ms with 200 μM PB.

The analysis of the channel closed times was complicated by the number of components in the closed time histograms and the simultaneous, competing actions of PB on the receptor activation – a decrease in the mean closed time duration due to an increased effective opening rate, and an increase in the mean closed time duration due to channel block by PB. Hence, the identification of single-channel clusters in the records was hindered. The overall closed time histograms were best-fitted with the sum of four exponentials. We calculated the mean closed times for α4β2δ currents elicited by PB using the three shorter-lived closed time components and ignoring the longest-lived component which has a mean duration of >100 ms. The mean closed times were 5.2 ms with 40 μM PB, 3.3 ms with 100 μM PB and 4.3 ms with 200 μM PB. The initial reduction in the closed time duration probably results from an increase in the effective opening rate. The subsequent increase in the closed time duration is likely to

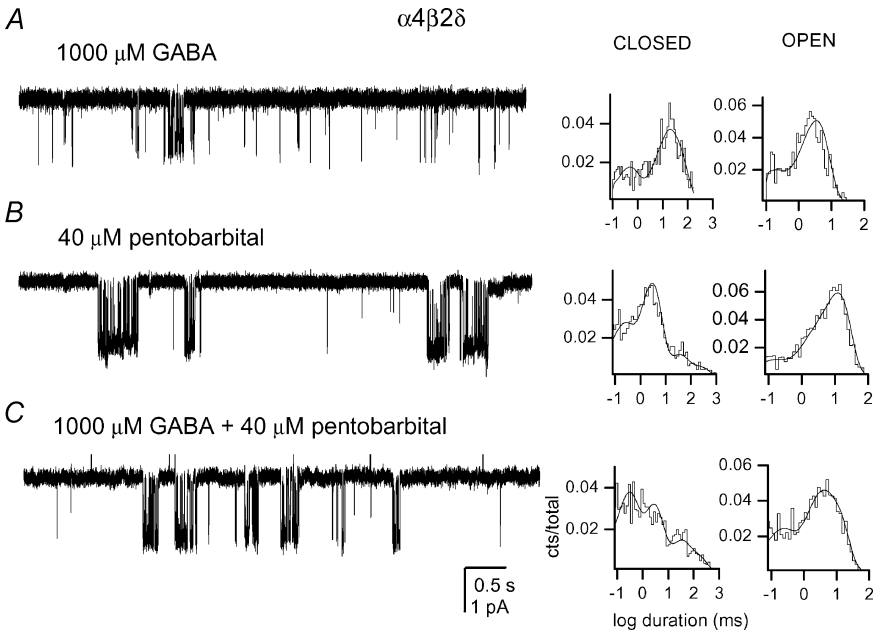

Figure 6. Single-channel currents from the α4β2δ $GABA_A$ receptor
The currents were elicited by 1000 μM GABA (*A*), 40 μM pentobarbital (*B*) or 1000 μM GABA + 40 μM PB (*C*). Channel openings are shown downward. The patch closed and open interval duration histograms are given next to the traces. The results of multi exponential fits are [duration (relative frequency)]: *A*: closed, 0.38 ms (26%), 11.1 ms (32%) and 37 ms (42%); open, 0.12 ms (22%) and 3.2 ms (78%); *B*: closed, 0.15 ms (24%), 2.5 ms (58%), 27 ms (12%) and 167 ms (7%); open, 0.1 ms (9%), 1.4 ms (13%) and 11 ms (77%); *C*: closed, 0.22 ms (39%), 2.3 ms (37%), 23 ms (14%) and 111 ms (10%); open, 0.15 ms (23%), 2 ms (30%) and 8.2 ms (48%). Due to rounding, the sum of weights may not equal 100%.

be due to increased channel block, as shown above for the $\alpha4\beta2\gamma2$ receptor activation by PB.

The effect of 40 μM PB on the activation of $\alpha4\beta2\delta$ receptors by 10–5000 μM GABA was also examined. Sample currents elicited by 1000 μM GABA in the absence and presence of 40 μM PB are shown in Fig. 6. To our surprise, the addition of GABA did not lead to an enhancement of receptor function. The open time histograms contained three components whose mean durations and relative weights were unaffected by changes in the concentration of GABA. The mean durations (relative frequencies) of the components at 10–5000 μM GABA, in the presence of 40 μM PB, were: for OT_1, 0.18 $\pm$ 0.08 ms (17 $\pm$ 7%); for OT_2, 2.4 $\pm$ 1.5 ms (28 $\pm$ 21%); for OT_3, 10.8 $\pm$ 1.7 ms (54 $\pm$ 23%). The open times were averaged from six patches, with a total number of events 20550. These values are similar to the open time parameters obtained at 40 μM PB, in the absence of GABA (see above). The data indicate that GABA and PB do not positively interact on the $\alpha4\beta2\delta$ receptor to prolong open times. This is in clear contrast to results found for $\alpha1\beta2\gamma2$ receptors, for which the combination of PB (50 μM) and GABA (10–1000 μM) resulted in a prolongation of the mean duration of the OT_3 component from 3.3 ms (PB alone) or 6.3 ms (GABA alone) to 13.3 ms.

Upon examining the channel closed times, we also failed to see an effect of GABA on currents elicited by 40 μM PB. The channel mean closed times were 4.8 ms with 10 μM GABA, 8.9 ms with 50 μM GABA, 5.9 ms with 100 μM GABA, 6.0 ms with 500 μM GABA, 4.5 ms with 1000 μM GABA, 4.2 ms with 2000 μM GABA and 4.1 ms with 5000 μM GABA. In all cases, 40 μM PB was coapplied with the specified concentration of GABA. Similarly to the analysis of currents elicited by PB alone (see above), we excluded the long-lived closed time component ($\tau >$ 100 ms) from this analysis.

Macroscopic currents from $\alpha4\beta2\delta$ receptors were examined in the presence of 1 mM GABA, or 100 or 1000 μM PB. Sample macroscopic responses, comparison of peak currents and residual currents (current levels at 5 s after peak, compared to peak value) are presented in Fig. 7. The results demonstrate that the peak amplitude in the presence of 100 μM PB is 3-fold greater than the amplitude of responses elicited by 1 mM GABA. The responses to 100 μM PB decayed quickly due to desensitization in the sustained presence of PB. The residual current at 5 s was only ~10% of the peak current. In comparison, the residual currents in the presence of 1 mM PB or 1 mM GABA were 40–60%. The results from whole-cell recordings agree with the single-channel studies demonstrating that PB is a more efficacious agonist than GABA on the $\alpha4\beta2\delta$ receptors, and that GABA-activated receptors desensitize more slowly than those activated by PB.

Discussion

Expression studies have suggested that receptors containing the δ subunit, and the $\alpha6$ or $\alpha4$ subunit are located in the extrasynaptic regions, and preferentially associated with tonic inhibition (Nusser *et al.* 1998). In contrast, the rapidly desensitizing synaptic currents are likely to be mediated by receptors containing $\alpha1$ and $\gamma2$ subunits (Nusser & Mody, 2002). It should be mentioned that the number of GABA-activated conductance classes is greater for extrasynaptic than synaptic $GABA_A$ receptors in cerebellar granule cells suggesting of higher degree of heterogeneity in receptor subunit composition

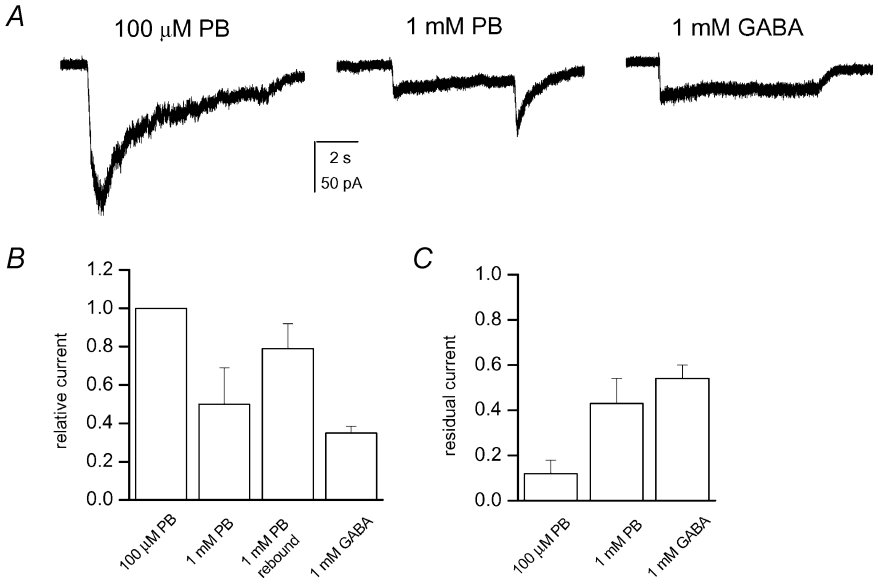

Figure 7. Macroscopic currents from HEK cells expressing $\alpha4\beta2\delta$ subunit receptors
A, the currents were elicited by 100 μM PB, 1 mM PB or 1 mM GABA. Rebound current in the end of the 1 mM PB application is caused by removal of PB-mediated block. *B*, normalized to peak current levels in the presence of 100 μM PB, the peak current for 1 mM PB was 0.5 $\pm$ 0.19 ($n = 4$), for 1 mM PB the rebound current was 0.79 $\pm$ 0.13 and the peak current for 1 mM GABA was 0.35 $\pm$ 0.03 ($n = 4$). *C*, residual current measured 5 s after the peak response is plotted, normalized to the peak response in that trace. The residual current level for 100 μM PB was 0.12 $\pm$ 0.06, for 1 mM PB it was 0.43 $\pm$ 0.11 and for 1 mM GABA it was 0.54 $\pm$ 0.06.

(Brickley *et al.* 1999). The currents associated with tonic (extrasynaptic) and phasic (synaptic) inhibition may have different roles. It has been proposed that the activation of extrasynaptic receptors controls the passive membrane properties, such as the cell input resistance affecting the time window for synaptic integration (Hausser & Clark, 1997). In rat cerebellar granule cells, the activation of synaptic GABA$_A$ receptors leads to an increased synchronicity in firing while tonic inhibition has the opposite effect (De Schutter, 2002). An increase in the concentrations of ambient GABA by tiagabine or vigabatrin potentiates tonic inhibition but reduces miniature and evoked IPSCs (Overstreet & Westbrook, 2001). Both these compounds have anticonvulsant properties, suggesting that activation and/or potentiation of extrasynaptic but not synaptic GABA$_A$ receptors underlie the treatment of certain types of seizures. Hence, discovery of site-specific pharmacological agents would be particularly useful.

Because of the differences in the subunit composition, it comes as no great surprise that the biophysical and pharmacological properties of synaptic and extrasynaptic receptors differ. In rat CA1 pyramidal neurones, extrasynaptic receptors demonstrate slower deactivation, compared to synaptic receptors, and the responses from extrasynaptic receptors are modulated by cytoplasmic calcium (Banks & Pearce, 2000). In hippocampal neurones, gabazine and penicillin inhibit mIPSCs but not the tonic current (Bai *et al.* 2001; Yeung *et al.* 2003). Also, midazolam and propofol, at clinical concentrations, have a greater effect on charge transfer during tonic current than mIPSCs (ibid.). On the other hand, in dentate gyrus granule cells, zolpidem potentiated synaptic receptors without affecting tonic inhibition (Nusser & Mody, 2002). Work on recombinant receptors containing the α4 subunit has shown them to be insensitive to benzodiazepines such as diazepam or flunitrazepam, setting such receptors apart from those containing the α1 subunit (Wieland *et al.* 1992; Brown *et al.* 2002). Receptors containing the α4 and δ subunits exhibit reduced desensitization (Brown *et al.* 2002), making them suitable for maintaining tonic inhibition. Recently, the ability of ethanol to potentiate GABA-elicited currents from α4β2δ receptors was demonstrated (Sundstrom-Poromaa *et al.* 2002).

Here, we have studied the activation of α4 subunit-containing receptors by GABA and pentobarbital. The α4 subunit was coexpressed with the β2, and γ2 or δ subunits. Both subunit combinations expressed receptors activatable by GABA and PB. The results from kinetic modelling demonstrate that GABA is a high affinity but a relatively low efficacy agonist for the α4β2γ2 receptor. The microscopic affinity of the resting α4β2γ2 receptor to GABA is about 20 μM. This value is similar to the estimates for the affinity of GABA$_A$ receptors containing the α1 subunit (Haas & Macdonald, 1999; Li & Pearce, 2000). The channel opening rate constant is 250 s^{-1}. Hence, the substitution of the α1 by the α4 subunit reduces the channel opening rate constant by almost 10-fold (Steinbach & Akk, 2001). This effect was not accompanied by changes in the general pattern of receptor activation, as the number of open and closed states in the records and their overall properties were unaffected (ibid.).

The EC$_{50}$ of the α4β2γ2 receptor cluster P_o curve (32 μM) is approximately 10-fold higher than EC$_{50}$ values for whole-cell dose–response curves estimated for recombinant α4β3γ2 receptors (Brown *et al.* 2002) or native receptors responsible for tonic currents in mouse hippocampal neurones (Yeung *et al.* 2003). The disagreement may arise from differences in subunit composition or expression system. We have not pursued this issue further.

In contrast, the activation of α4β2δ receptors by GABA was not characterized by single-channel clusters. Instead, persisting, non-desensitizing currents (isolated openings and short bursts) were seen at GABA concentrations up to 1 mM. Changes in GABA concentration did not affect noticeably the channel closed durations. In the whole-cell recordings, currents from α4β3δ receptors are also characterized by slow desensitization (Brown *et al.* 2002). This pattern of behaviour is similar to currents from receptors containing α1βδ subunits (α1β2δ, G. Akk, unpublished observations; α1β3δ, Haas & Macdonald, 1999). We speculate that reduced desensitization of receptors containing the δ subunit leads to such persisting currents while a dominating, long-lived closed state in the single-channel records masks the agonist-dependent CT$_\beta$ component. The origin of the long-lived closed state is unclear but a prominent, frequently visited closed state which rapidly equilibrates with the open states would agree with the experimental findings.

Our results show that PB is a strong activator of α4 containing receptors. In the single-channel recordings, the maximal open probability of receptors containing the α4 and β2 subunits, and either the γ2 or the δ subunit was greater in the presence of PB than GABA. The open probability was greatest at 100–200 μM, while at higher concentrations of PB the open probability was reduced due to channel block. Channel block was manifested as both a reduction in the mean open duration as well as an increase in the mean closed time duration. In the α4β2γ2 receptor, the rate of entry into the blocked state, determined from the reduction in the mean open time

durations, was similar to the blocking rate in the $\alpha1\beta2\gamma2$ receptor (Akk & Steinbach, 2000).

Interestingly, in $\alpha4\beta2\delta$ receptors, the addition of GABA had no effect on currents (open or closed time durations) elicited by 40 μM PB. Earlier studies on the recombinant $\alpha1\beta2\gamma2$ receptor have shown that the coapplication of GABA and PB results in an increase in the mean open time duration over that seen in the presence of either GABA or PB alone (Akk & Steinbach, 2000; Steinbach & Akk, 2001). In the present case, the channel open times were fully determined by PB, and the addition of GABA had no further effect. It is not immediately clear how to account for this finding. It is possible that the channel activation was saturated by 40 μM PB. However, the observation that the mean closed time within clusters decreased between 40 μM and 100 μM PB suggests that this is not the case. Alternatively, it is possible that channel block could obscure potentiation.

It is generally accepted that the agonistic properties of GABA and PB are mediated via separate sites (Amin & Weiss, 1993; Ueno *et al.* 1997). Our findings are clearly consistent with GABA and PB binding to distinct domains as PB-mediated activation was not inhibited by GABA acting as a low-efficacy agonist, even at 5 mM. Further studies will have to be carried out to investigate the modulatory properties of barbiturates. The concentration of pentobarbital used in these experiments is similar to the concentrations measured in brains of anaesthetized animals ($\sim$100 μM, Saubermann *et al.* 1974). Hence, if pentobarbital-mediated anaesthetic effects are due to interactions with the $\alpha4\beta2\delta$ receptor, such interactions would probably be mediated via direct activation of the receptor by pentobarbital, not by potentiation of GABA-activated currents.

Strong direct activation of $\alpha4$-containing receptors by PB was unexpected as a previous study had demonstrated a lack of direct activation of $\alpha4\beta1\gamma2$ receptors by PB (Wafford *et al.* 1996). We do not have an explanation for this discrepancy between our data and the results obtained previously. To test the unlikely possibility that the difference among the β subunits used in these two studies is responsible for the inconsistency, we examined the activation of $\alpha4\beta1\gamma2$ receptors by GABA and PB. In this combination, the open probability of receptors was 0.33 when activated by 1 mM GABA, and 0.66 in the presence of 100 μM PB (data not shown). Similarly to $\beta2$ subunit-containing receptors, the cluster open probability decreased when the concentration of PB was further increased to 1 mM. Therefore, the nature of the β subunit did not affect the activation (or block) by PB. We also examined whether differences in the expression system may affect responses to PB (oocytes were used by Wafford *et al.* 1996 *versus* HEK cells in the present study). Our results indicate that $\alpha4\beta1\gamma2$ receptors expressed in *Xenopus* oocytes are responsive to PB (data not shown). Finally, the species difference may be responsible for the lack of direct activation by PB in Wafford *et al.* (1996), who used fully human receptors. In the present study, the human $\alpha4$ subunit was used along with rat β and $\gamma2$ or δ subunits.

In conclusion, the results presented in this manuscript demonstrate that $\alpha4\beta2\gamma2$ and $\alpha4\beta2\delta$ receptors are activated by GABA and PB. The strong responses seen in the presence of PB suggest a role for $\alpha4$ subunit-containing receptors in PB-mediated effects in the mammalian nervous system. The presumed extrasynaptic location of the $\alpha4\beta2\delta$ receptors makes these receptors an attractive target of barbiturates in controlling tonic inhibitory conductance.

References

Adkins CE, Pillai GV, Kerby J, Bonnert TP, Haldon C, McKernan RM, Gonzalez JE, Oades K, Whiting PJ & Simpson PB (2001). $\alpha4\beta3\delta$ $GABA_A$ receptors characterized by fluorescence resonance energy transfer-derived measurements of membrane potential. *J Biol Chem* **276**, 38934–38939.

Akaike N, Maruyama T & Tokutomi N (1987). Kinetic properties of the pentobarbitone-gated chloride current in frog sensory neurones. *J Physiol* **394**, 85–98.

Akk G (2002). Contributions of the non-α subunit residues (loop D) to agonist binding and channel gating in the muscle nicotinic acetylcholine receptor. *J Physiol* **544**, 695–705.

Akk G & Steinbach JH (2000). Activation and block of recombinant $GABA_A$ receptors by pentobarbitone: a single-channel study. *Br J Pharmacol* **130**, 249–258.

Amin J & Weiss DS (1993). $GABA_A$ receptor needs two homologous domains of the β ssubunit for activation by GABA but not by pentobarbital. *Nature* **366**, 565–569.

Bai D, Zhu G, Pennefather P, Jackson MF, MacDonald JF & Orser BA (2001). Distinct functional and pharmacological properties of tonic and quantal inhibitory postsynaptic currents mediated by γ-aminobutyric $acid_A$ receptors in hippocampal neurons. *Mol Pharmacol* **59**, 814–824.

Banks MI & Pearce RA (2000). Kinetic differences between synaptic and extrasynaptic. $GABA_A$ receptors in CA1 pyramidal cells. *J Neurosci* **20**, 937–948.

Baumann SW, Baur S & Sigel E (2001). Subunit arrangement of γ-aminobutyric acid type A receptors. *J Biol Chem* **276**, 36275–16280.

Brickley SG, Cull-Candy SG & Farrant M (1999). Single-channel properties of synaptic and extrasynaptic $GABA_A$ receptors suggest differential targeting of receptor subtypes. *J Neurosci* **19**, 2960–2973.

Brown N, Kerby J, Bonner TP, Whiting PJ & Wafford KA (2002). Pharmacological characterization of a novel cell line expressing human $\alpha 4\beta 3\delta$ $GABA_A$ receptors. *Br J Pharmacol* **136**, 965–974.

Chang Y, Wang R, Barot S & Weiss D (1996). Stoichiometry of a recombinant $GABA_A$ receptor. *J Neurosci* **16**, 5415–5424.

De Schutter E (2002). Cerebellar cortex: computation by extrasynaptic inhibition? *Curr Biol* **12**, R363–R365.

Fisher JL & Macdonald RL (1997). Single channel properties of recombinant $GABA_A$ receptors containing $\gamma 2$ or δ subtypes expressed with $\alpha 1$ and $\beta 3$ subtypes in mouse L929 cells. *J Physiol* **505**, 283–297.

Fletcher GH & Steinbach JH (1996). Ability of nondepolarizing neuromuscular blocking drugs to act as partial agonists at fetal and adult mouse muscle nicotinic receptors. *Mol Pharmacol* **49**, 938–947.

Haas KF & Macdonald RL (1999). $GABA_A$ receptor subunit $\gamma 2$ and δ subtypes confer unique kinetic properties on recombinant $GABA_A$ receptor currents in mouse fibroblasts. *J Physiol* **514**, 27–45.

Hamill OP, Marty A, Neher E, Sakmann B & Sigworth FJ (1981). Improved patch-clamp techniques for high-resolution current recording from cells and cell-free membrane patches. *Pflugers Arch* **391**, 85–100.

Hausser M & Clark BA (1997). Tonic synaptic inhibition modulates neuronal output pattern and spatiotemporal synaptic integration. *Neuron* **19**, 665–678.

Horn R (1987). Statistical methods for model discrimination. Applications to gating kinetics and permeation of the acetylcholine receptor channel. *Biophys J* **51**, 255–263.

Jones MV & Westbrook GL (1995). Desensitized states prolong $GABA_A$ channel responses to brief agonist pulses. *Neuron* **15**, 181–191.

Li X & Pearce RA (2000). Effects of halothane on $GABA_A$ receptor kinetics: evidence for slowed agonist unbinding. *J Neurosci* **20**, 899–907.

Newland CF, Colquhoun D & Cull-Candy SG (1991). Single channels activated by high concentrations of GABA in superior cervical ganglion neurones of the rat. *J Physiol* **432**, 203–233.

Nusser Z & Mody I (2002). Selective modulation of tonic and phasic inhibitions in dentate gyrus granule cells. *J Neurophysiol* **87**, 2624–2628.

Nusser Z, Sieghart W & Somogyi P (1998). Segregation of different GABAA receptors to synaptic and extrasynaptic membranes of cerebellar granule cells. *J Neurosci* **18**, 1693–1703.

Overstreet LS & Westbrook GL (2001). Paradoxical reduction of synaptic inhibition by vigabatrin. *J Neurophysiol* **86**, 596–603.

Puia G, Santi M, Vicini S, Pritchett DB, Purdy RH, Paul SM, Seeburg PH and Costa E (1990). Neurosteroids act on recombinant human GABAA receptors. *Neuron* **4**, 759–765.

Qin F, Auerbach A & Sachs F (1996). Estimating single-channel kinetic parameters from idealized patch-clamp data containing missed events. *Biophys J* **70**, 264–280.

Qin F, Auerbach A & Sachs F (1997). Maximum likelihood estimation of aggregated Markov processes. *Proc R Soc Lond B* **264**, 375–383.

Rudolph U, Crestani F & Mohler H (2001). $GABA_A$ receptor subtypes: dissecting their pharmacological functions. *Trends Pharm Sci* **22**, 188–194.

Saubermann AJ, Gallagher ML & Hedley-White J (1974). Uptake, distribution and anesthetic effect of pentobarbital-2–^{14}C after intravenous injection into mice. *Anesthesiology* **40**, 41–51.

Serafini R, Bracamontes J & Steinbach JH (2000). Structural domains of the human $GABA_A$ receptor $\beta 3$ subunit involved in the actions of pentobarbital. *J Physiol* **524**, 649–676.

Steinbach JH & Akk G (2001). Modulation of $GABA_A$ receptor gating by pentobarbital. *J Physiol* **537**, 715–733.

Sundstrom-Poromaa I, Smith DH, Gong QH, Sabado TN, Li X, Light A, Wiedmann M, Williams K & Smith SS (2002). Hormonally regulated $\alpha 4\beta 2\delta$ $GABA_A$ receptors are a target for alcohol. *Nature Neurosci* **5**, 721–722.

Sur C, Farrar SJ, Kerby J, Whiting PJ, Atack JR & McKernan RM (1999). Preferential coassembly of $\alpha 4$ and δ subunits of the γ-aminobutyric acid (A) receptor in rat thalamus. *Mol Pharmacol* **56**, 110–115.

Twyman RE, Rogers CJ & Macdonald RL (1990). Intraburst kinetic properties of the $GABA_A$ receptor main conductance state of mouse spinal cord neurones in culture. *J Physiol* **423**, 193–220.

Ueno S, Bracamontes J, Zorumski C, Weiss DS & Steinbach JH (1997). Bicuculline and gabazine are allosteric inhibitors of channel opening of the $GABA_A$ receptor. *J Neurosci* **17**, 625–634.

Wafford KA, Thompson SA, Thomas D, Sikela J, Wilcox AS & Whiting PJ (1996). Functional characterization of human γ-aminobutyric acidA receptors containing the $\alpha 4$ subunit. *Mol Pharmacol* **50**, 670–678.

Wieland HA, Luddens H & Seeburg PH (1992). A single histidine in $GABA_A$ receptors is essential for benzodiazepine agonist binding. *J Biol Chem* **267**, 1426–1429.

Wisden W, Laurie DJ, Monyer H & Seeburg PH (1992). The distribution of 13 $GABA_A$ receptor subunit mRNAs in the rat brain. I. Telencephalon, diencephalon, mesencephalon. *J Neurosci* **12**, 1040–1062.

Yeung JY, Canning KJ, Zhu G, Pennefather P, MacDonald JF & Orser BA (2003). Tonically activated $GABA_A$ receptors in hippocampal neurons are high-affinity, low-conductance sensors for extracellular GABA. *Mol Pharmacol* **63**, 2–8.

Acknowledgements

We thank Jessie Zhang and Sarah Hamm for tissue culture work. This work was supported by the Alcoholic Beverage Medical Research Foundation (G.A.) and NIH PO1 G47969 (J.H.S.).